EGG--2050

Distribution Category: DE91 015629

MEAN STRESS EFFECTS ON HIGH-CYCLE FATIGUE OF ALLOY 718

Gary E. Korth

Published July 1980

EG&G Idaho, Inc
Idaho Falls, Idaho 83415

Prepared for the
U.S. Department of Energy
Idaho Operations Office
Under DOE Contract No. DE-AC07-76ID01570

DISCLAIMER

ABSTRACT

This report covers an investigation of the effects of tensile mean stress on the high-cycle fatigue properties of Alloy 718 . Three test temperatures (24, 427, and 649°C) were employed, and there were tests in both strain and load control. Results were compared with three different models: linear Modified-Goodman, Peterson cubic, and stress-strain parameter. The linear Modified-Goodman model gave good correlation with actual test data for low and moderate mean stress values, but the stress-strain parameter showed excellent correlation over the entire range of possible mean stresses and therefore is recommended for predicting mean stress effects of Alloy 718.

ACKNOWLEDGMENTS

This investigation was made possible by the Department of Energy, Division of Reactor Research and Technology (DOE-RRT). The author is indebted to J. V. Burch and M. D. Harper for conducting the tests and A. L. Snow of Westinghouse (Advanced Reactors Division) for assistance with the modeling analysis.

CONTENTS

Abstract ii

Acknowledgments iii

Introduction 1

Materials 1

Test Details 1

Results 2

Mean Stress Models 2

Conclusions 15

References 16

FIGURES

1. Stress-strain representation of fatigue cycling when stresses are totally elastic, without mean stress (a), and mean stress, S_m (b) 5

2. Mean stress versus cycles for Alloy 718 fatigue tested at 649°C in load control with three levels of mean stress, showing ratcheting (cyclic creep). Test specimens 214-14, 214-48, and 214-49 5

3. Strain-controlled fatigue test of Alloy 718 at 649°C with mean strain, showing cylic relaxation. Test specimen 214-4 6

4. Hysteresis loops of strain-controlled inelastic fatigue without mean strain (a) and with mean strain (b), with the same strain range $\Delta\epsilon_t$ 6

5. Modified-Goodman diagram for correcting stress amplitude due to mean stress 7

6. Stress-strain curves for heats 6 and R at 427°C comparing cyclic and monotonic behavior 8

7. Hysteresis loops of Alloy 718 strain-controlled fatigue tests with mean strain. Test temperature: 427°C 9

8. Strain-controlled fatigue of Alloy 718 at 427°C showing effects of mean strain on stress range and cycle life 10

9. Mean stress fatigue data of Alloy 718 compared to the Peterson cubic and the Modified-Goodman linear models 13

10. Mean stress fatigue data of Alloy 718 compared to the stress-strain model 14

11. Comparison of actual fatigue test data of Alloy 718 at 427°C with stress-strain parameter predictions 14

12. Stress amplitude reduction versus maximum stress for Alloy 718 mean stress tests 15

TABLES

1. Alloy 718 material for mean stress effects tests 2

2. Alloy 718 mean stress load control fatigue data 3

3. Alloy 718 strain control fatigue data with mean strain 4

4. Material properties used in mean stress evaluations 13

MEAN STRESS EFFECTS ON HIGH CYLCE FATIGUE OF ALLOY 718

INTRODUCTION

High-cycle fatigue behavior is an important design consideration of some components and subcomponents of sodium-cooled nuclear reactors that are subject to a phenomenon termed "thermal striping." This condition exists in areas where sodium streams of significantly different temperatures mix and impinge on the surfaces of the surrounding structural components. These surfaces are therefore subjected to fluctuating hot and cold sodium, giving rise to thermal stresses of enough magnitude to initiate high-cycle fatigue surface cracks that could grow and eventually cause component failure. Fluctuations are likely to be of the order of 1 Hz and therefore a permanent component could suffer thermal stress cycles of the order of 10^9 over its intended thirty-year life.

Austenitic stainless steels (Types 304 and 316) have historically been selected for the structural components of sodium-cooled reactors, but the high-cycle fatigue properties of these materials require that temperature fluctuations be limited to less than 60°C (~ 30°C with design safety factors). This requirement puts severe operating restrictions on large energy-producing systems.

One solution to the thermal striping problem is to use Alloy 718 in areas where high thermal stresses are expected. This material has significantly better high-cycle fatigue properties and with its thermal expansion advantage allows temperature fluctuation amplitudes of approximately five times the values possible with Types 304 and 316 stainless steels. However, Alloy 718, as a high-strength superalloy, has a relatively high yield-to-ultimate-strength ratio and exhibits its high-cycle fatigue strength in the elastic regime. It is therefore subject to fatigue strength reductions due to mean stress effects, a problem which partially offsets its advantage over the stainless steels.

Mean stress can result from any number of sources, including forming operations during fabrication, mismatch conditions during assembly, welding stresses, locked-in heat-treat stresses, surface-finishing techniques, or static preloads due to service conditions. This paper addresses the effects of mean stress on the high-cycle fatigue behavior of Alloy 718 and compares actual data with some proposed mathematical models.

MATERIALS

Test specimens came from Alloy 718 plate of 12.7 to 19.1-mm thickness. Five heats of material represent the baseline data (mean stress = 0) and three heats were tested with mean stresses. The materials are identified in Table 1.

All materials reported herein were given the following conventional heat treatment:

- 954°C solution annealed for 1 hour
- air cooled
- aged at 718°C for 8 hours
- furnace cooled at 55°C/hour to 621°C
- aged at 621°C until total aging time is 18 hours
- air cooled.

TEST DETAILS

There were two kinds of tests:

1. Baseline tests (zero mean stress) from 10^2 to 10^6 cycles-to-fail in the strain control mode, using axially loaded hourglass-shaped specimens with a minimum diameter of 5.08 mm.

2. Baseline tests from 3×10^4 to 10^9 cycles-to-fail in the load control mode using axial hourglass specimens of the same geometry as used in the strain control tests and also rotating beam specimens with minimum diameters of either 5.08 or 6.35 mm. The hourglass radius of curvature was ten times the minimum diameter for the axial specimens and between ten and forty times for the rotating beam specimens.

TABLE 1. ALLOY 718 MATERIAL-MEAN STRESS EFFECTS TEST

EG&G Designation	Manufacturer's Identification	Product Form	Reference for Chemistry Details
Heat 1	2180-2-9251	15.9-mm plate	1
Heat 2	2180-2-9247	19.1-mm plate	1
Heat 3	52C9EK	12.7-mm plate	1
Heat 6	2180-4-9478	12.7-mm plate	2
Heat R[a]	2180-6-9458	19.1-mm plate	2

a. Alloy 718 reference heat.

There were mean stress tests in both modes with 5.08-mm diameter, axially loaded hourglass specimens. The elevated temperature tests took place in an air environment using induction heating techniques.

RESULTS

The baseline data have been reported elsewhere[1-7] and are not repeated in this report. The load control mean stress test results are in Table 2, and the strain control mean strain test results are in Table 3. The test data in Table 2 represent essentially all elastic behavior during cycling. There were, however, a number of cases where the peak stress (stress amplitude, S_{eq}, plus mean stress, S_m) was greater than the proportional limit, S_p, which resulted in some yielding on the first quarter-cycle; but all subsequent cycling was fully elastic except for three 649°C tests (Specimens 214-14, 214-48, and 214-49) where there was some ratcheting. The data presented in Table 3 include a number of tests where a small inelastic strain persisted throughout the test.

MEAN STRESS MODELS

When loading stresses are totally elastic with a stress ratio, A, (= stress amplitude/mean stress, S_{eq}/S_m) of infinity, i.e., $S_m = 0$, then the resulting stress-strain behavior is represented by Figure 1a. However, when a tensile mean stress is present, then the peak stress shifts upward by an amount equal to the mean stress, S_m (Figure 1b).

Even though the stress amplitude, S_{eq}, remains the same, the cyclic life is shortened because of the increased peak stress. When temperatures are below the creep regime, the mean stress and strain should remain constant; whereas when service temperatures are high enough for creep to be significant, the mean strain should increase (ratchet) in a load-controlled condition or the stress would relax when the loading is strain controlled.

These phenomena have been observed, and results for a test temperature of 649°C are illustrated in Figures 2 and 3. When the cyclic loading is in the inelastic range, the behavior should be similar to high-temperature elastic behavior (ratcheting and relaxation for load- and strain-controlled loadings, respectively). An example of starting strain-controlled hysteresis loops is shown in Figure 4 for no mean strain (a) and with mean tensile strain (b), when the strain range, $\Delta\epsilon_t$, is identical. After the first quarter cycle of the mean strain test is completed, the hysteresis loop becomes almost identical to the loop without mean strain, and after a few more cycles, the tensile stress should relax to a point where the mean strain would no longer be perceptible at all except for the initial offset.

TABLE 2. ALLOY 718 MEAN STRESS LOAD CONTROL FATIGUE DATA

Specimen Number[a]	Test Temperature (°C)	Stress Amplitude, S_a (MPa)	Mean Stress, S_m (MPa)	Test Frequency (Hz)	Cycles to Fail N_f	S_{max}/S_p[b]
214-12	24	448	517	10	148,620	1.00
213-42	24	448	396	0.8	451,054	0.88
213-3	24	448	358	10	3,747,200	0.84
R10-17	24	363	537	30	3,000,240[c]	1.00
R10-35	24	363	537	30	6,118,200	1.00
623-89	427	552	276	10	99,660	1.00
623-75	427	552	241	10	171,130	0.96
623-91	427	552	138	10	421,950	0.83
623-95	427	517	310	10	153,260	1.00
R1-18	427	517	241	30	185,760	1.00
623-96	427	517	241	10	279,790	0.92
623-82	427	517	172	10	352,970	0.83
623-102	427	517	103	10	772,530	0.75
R1-16	527	482	276	30	297,000	1.00
R10-15	427	482	275	30	264,600	1.00
R11-26	427	460	200	30	1,130,278[c]	0.80
R10-20	427	453	367	30	279,720	1.08
R1-6	427	448	310	30	370,440	1.00
R11-33	427	435	625	30	192,190	1.39
R10-27	427	425	395	30	143,640	1.00
R10-12	427	425	395	30	266,760	1.00
R10-6	427	423	452	30	264,360	1.15
R12-26	427	414	345	30	697,680	1.00
R1-4	427	414	310	30	805,680	0.95
R1-14	427	414	241	30	1,154,520	0.86
R1-5	427	414	172	30	2,236,680	0.77
R1-15	427	414	172	30	3,994,160	0.77
R3-4	427	414	103	30	10,389,600	0.68
R3-16	427	414	69	30	89,262,640[c]	0.64
R10-22	427	391	537	30	319,680	1.22
R6-29	427	379	379	20	843,840	1.00
R11-31	427	358	613	30	702,000	1.28
R6-21	427	345	414	20	1,880,640	1.00
R11-27	427	340	530	30	924,065	1.15
R10-7	427	330	487	30	962,280	1.08
R11-9	427	325	599	30	746,544	1.22
R6-5	427	310	448	20	2,864,160	1.00
R8-36	427	310	448	30	10,670,406	1.00
R7-38	427	310	448	30	17,626,680[c]	1.00
R11-14	427	308	667	30	668,972	1.29
R7-21	427	303	455	30	94,053,960[c]	1.00
R11-8	427	300	740	30	841,320	1.37
R7-31	427	293	465	30	93,193,200[c]	1.00
R10-30	427	282	592	30	2,511,000	1.15
R11-12	427	280	792	30	1,397,206	1.42
R6-44	427	276	483	30	90,256,680[c]	1.00
R11-3	427	260	895	10	1,930,249	1.52
R11-7	427	250	951	10	5,192,859[c]	1.58
R11-39	427	240	684	30	64,122,840[c]	1.22
R11-24	427	200	913	30	74,689,882[c]	1.34
R11-29	427	200	771	30	53,510,760[c]	1.28
R3-9	649	483	241	30	277,560	1.00
214-14	649	448	517	0.36	327,674[d]	1.17
214-48	649	448	448	0.36	699,674[d]	1.08
214-49	649	448	379	0.36	990,010[c,d]	1.00
R1-13	649	448	276	30	174,280	1.00
R1-12	649	414	310	30	696,680	1.00
R8-38	649	414	207	30	4,079,160	0.86
R24-2	649	407	214	30	2,472,120	0.86
R1-22	649	407	214	30	2,675,160	0.86
R24-7	649	400	221	30	1,879,200	0.86
R24-8	649	400	221	30	7,565,400	0.86
R8-41	649	396	224	30	70,903,080[c]	0.86
R3-40	649	379	345	30	433,080	1.00
R3-31	649	345	379	30	2,237,760	1.00

a. Specimen Number RXX-XX = Reference Heat
6XX-XX = Heat 6
2XX-XX = Heat 2.

b. S_{max} = stress amplitude + mean stress, S_p = proportional limit.

c. Test terminated before failure.

d. Ratcheting observed (See Figure 2).

TABLE 3. ALLOY 718 STRAIN CONTROL FATIGUE DATA WITH MEAN STRAIN

Specimen Number[a]	Test Temperature (°C)	Total Strain Range (%)	Mean Tensile Strain (%)	Properties at $N_f/2$			Strain Rate (s^{-1})	Cycles to Fail (N_f)
				Plastic Strain (%)	Stress Amplitude (MPa)	Mean Stress (MPa)		
215-20	24	0.44	0.26	0.00	439	519	0.004	119,214
214-2	24	0.44	0.22	0.00	439	439	0.009	154,839
R9-14	24	0.70	0.10	0.08	770	5	0.004	43,100
R9-39	24	0.70	0.06	0.02	729	83	0.004	125,569
R9-22	24	0.70	0.08	0.02	718	147	0.004	73,400
R9-2	24	0.70	0.15	0.03	715	255	0.004	50,311
R9-30	24	0.70	0.20	0.02	716	269	0.004	45,614
R20-20	427	0.86	0.04	0.02	716	[b]	0.004	648,565
R20-7	427	0.86	0.04	0.01	720	40	0.004	49,390
R10-24	427	0.86	0.08	0.03	708	[b]	0.004	362,152
R10-37	427	0.86	0.16	0.01	703	79	0.004	147,582
R10-41	427	0.86	0.20	0.01	688	119	0.004	90,568
R10-28	427	0.87	0.12	0.01	729	[b]	0.004	106,761
625-46	427	1.00	1.00	0.08	773	148	0.004	9,504
614-18	427	1.00	1.00	0.07	773	88	0.004	8,727
614-24	427	1.00	0.50	0.04	821	51	0.004	33,307
614-11	427	1.00	0.25	0.02	821	14	0.004	65,796
214-4	649	0.44	0.22	---	370	c	0.004	442,056[c]

a. Spec. Number: RXX-XX = Reference Heat
2XX-XX = Heat 2
6XX-XX = Heat 6.

b. Mean stress varied considerably during test and no one value would be representative.

c. Test terminated before failure, cyclic relaxation observed (see Figure 3).

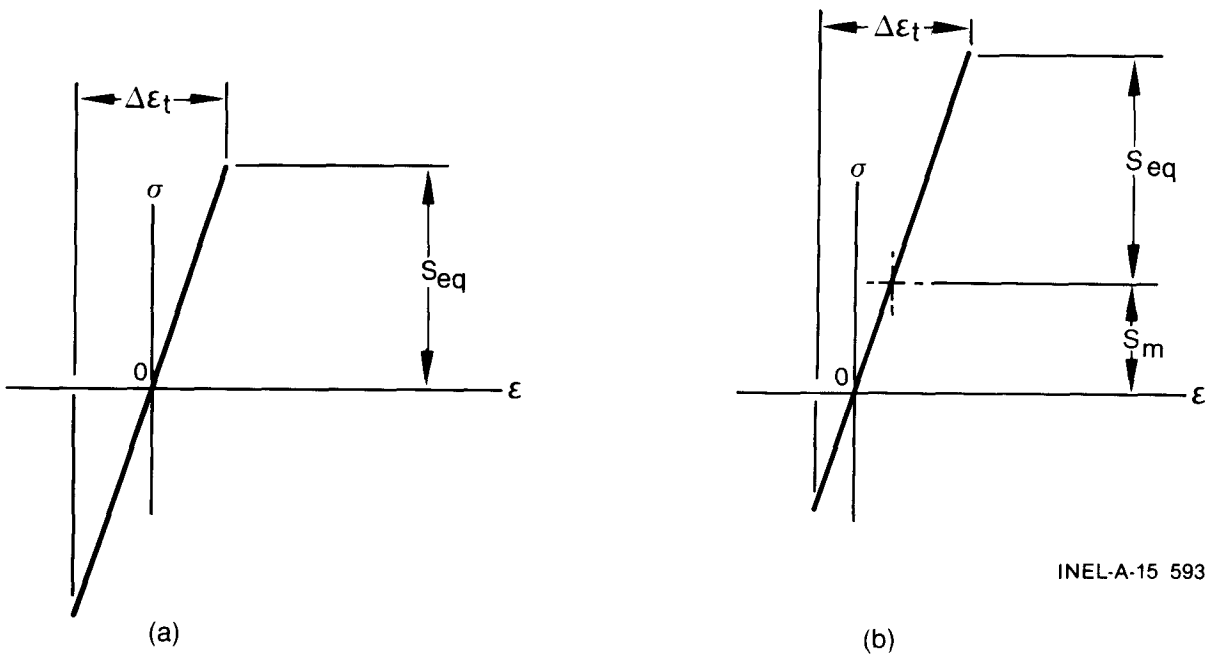

Figure 1. Stress-strain representation of fatigue cycling when stresses are totally elastic, without mean stress (a), and with mean stress, S_m (b).

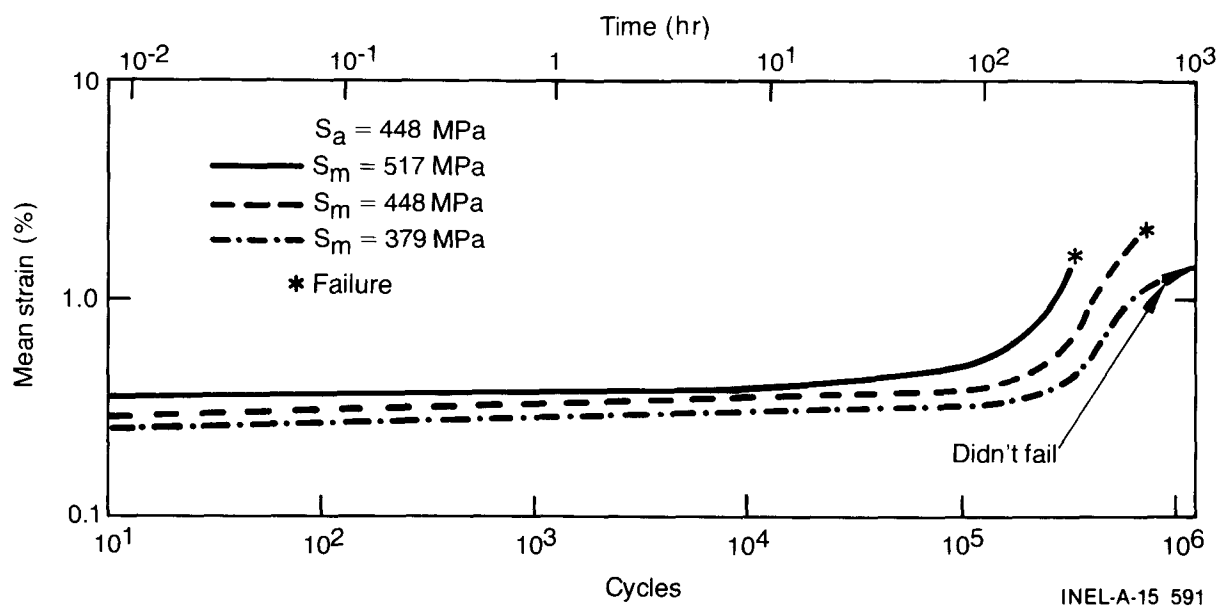

Figure 2. Mean stress versus cycles for Alloy 718 fatigue tested at 649°C in load control with three levels of mean stress, showing ratcheting (cyclic creep). Test specimens 214-14, 214-48, and 214-49.

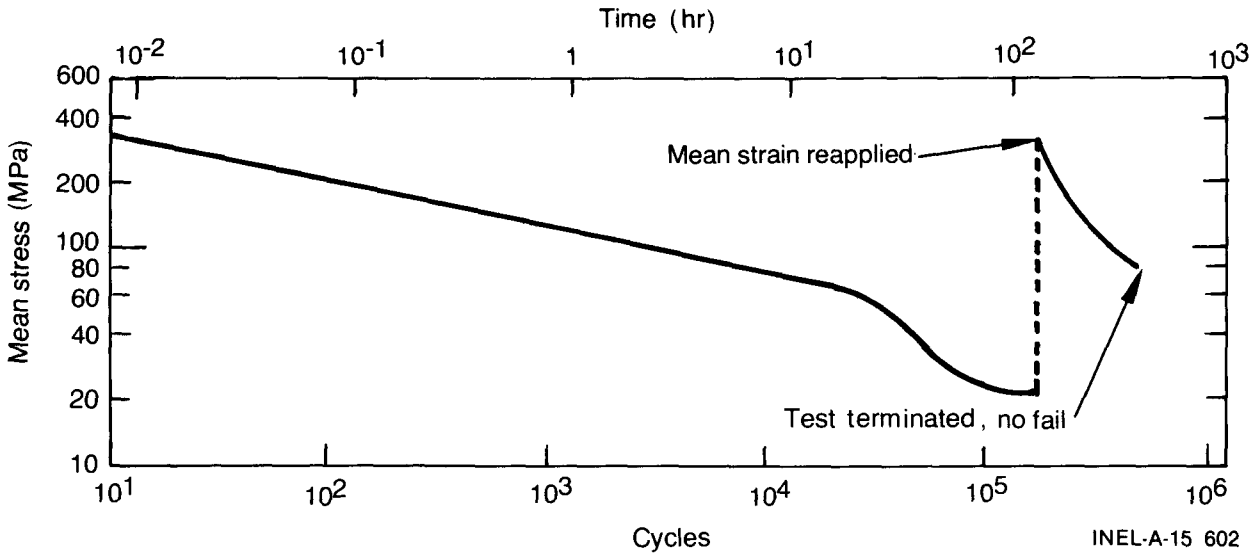

Figure 3. Strain-controlled fatigue test of Alloy 718 at 649°C with mean strain, showing cylic relaxation. Test specimen 214-14.

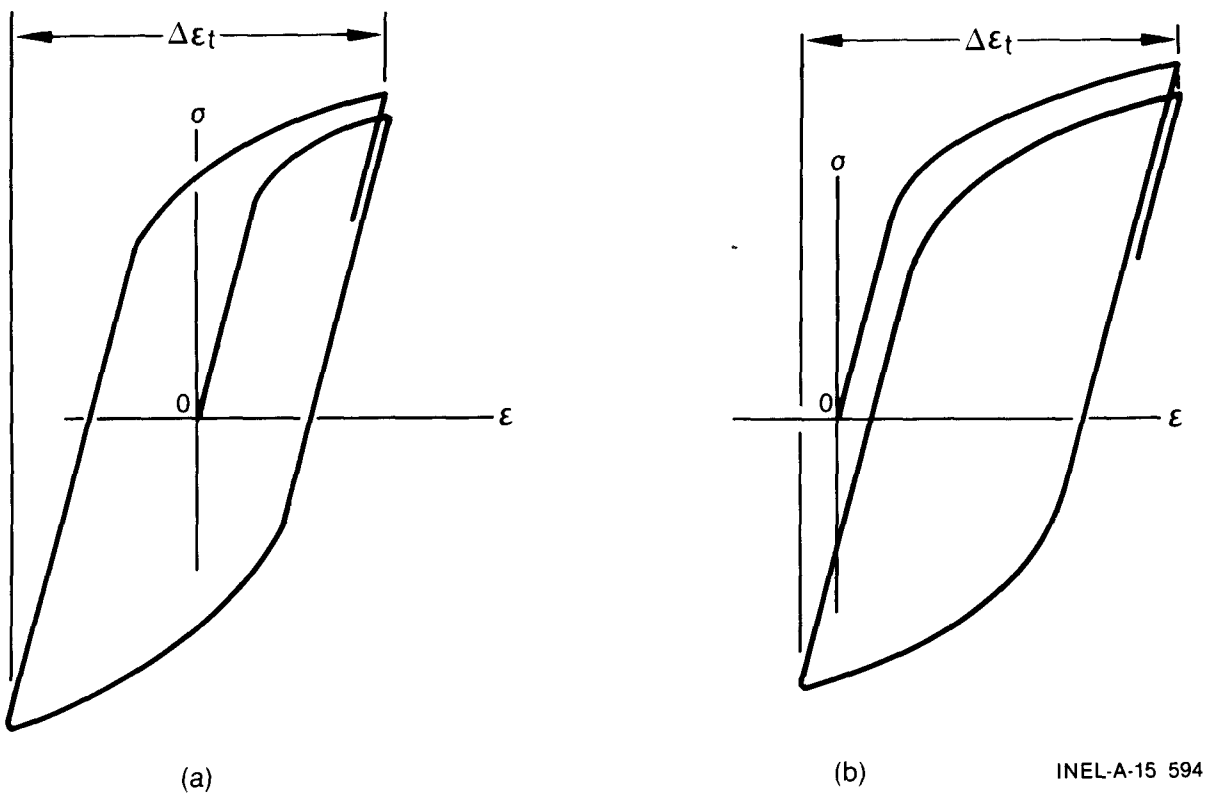

Figure 4. Hysteresis loops of strain-controlled inelastic fatigue without mean strain (a) and with mean strain (b), with the same strain range $\Delta\epsilon_t$.

The above reasoning is used to justify ignoring mean stress effects in a strain-controlled situation when strains are inelastic, and accounting for mean stress only when the loads are totally elastic. Using this reasoning, Langer[8] recommends the Modified-Goodman diagram (Figure 5) for correcting the stress amplitude for mean stress in elastic fatigue cycling where:

S_e = endurance limit
S_b = cyclic yield stress
S_u = ultimate stress
S_e' = adjusted endurance stress

When the mean stress (S_m) increases such that the sum $S_m + S_e = S_b$ extends beyond point C in the diagram, any further increase in S_m will result in yielding and the mean stress will revert back to C. In this situation, a mean stress of C′ is the maximum possible. From the geometry of Figure 5, the resulting adjusted endurance stress becomes:

$$S_e' = S_e \left[\frac{S_u - S_b}{S_u - S_e}\right]. \quad (1)$$

For a finite number of cycles, S_e becomes the stress amplitude, S_{eq}, as long as $S_{eq} = S_b$, or,

$$S_a = S_{eq} \left[\frac{S_u - S_b}{S_u - S_{eq}}\right] \quad (2)$$

where S_a is the stress amplitude corrected for mean stress.

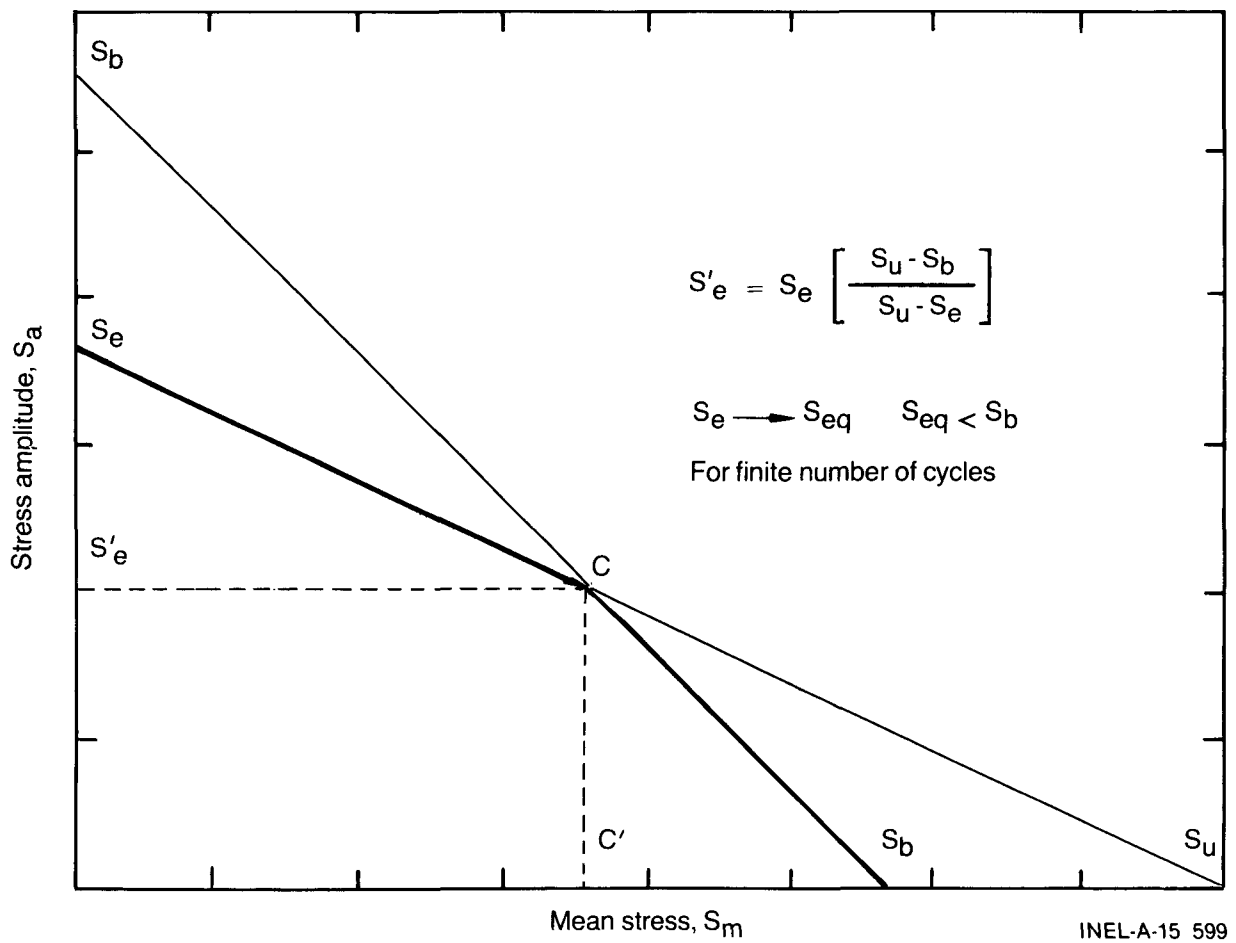

Figure 5. Modified-Goodman diagram for correcting stress amplitude due to mean stress.

Therefore, according to Langer, the worst case should be when the peak stress (S_{eq} + S_m) is just bumping the cyclic yield stress, S_b. Choosing a value for S_b often poses somewhat of a problem. If the monotonic 0.2% yield strength is selected (a conservative approach), then the resulting calculations for worst case show that the high-cycle fatigue behavior of Alloy 718 is no better than the austenitic stainless steels. A more realistic approach, and not nearly so severe, would be to equate S_b to the monotonic proportional limit or perhaps to a 0.2% yield of an actual cyclic stress-strain curve. Figure 6 gives a comparison of monotonic and cyclic stress-strain curves for 427°C.

Since Alloy 718 is a cyclic softening material, the cyclic stress-strain curve falls below the monotonic curve. Using the cyclic proportional limit for S_b would be much more realistic and would not impose such a severe penalty on the high-cycle fatigue strength. Typical calculations for Alloy 718 show a stress amplitude reduction of 0.43 when the cyclic 0.2% yield strength was used for S_b, and 0.65 when the monotonic proportional limit value was used. Using the Modified-Goodman correction, Jaske and O'Donnell[9] obtained stress amplitude reductions of up to 0.39 when using a room-temperature cyclic yield of 1014 Mpa.

There are some problems with the Modified-Goodman model and its worst-case assumptions and calculations. First is the difficulty in selecting a cyclic yield value which is truly representative of material behavior. This difficulty is alluded to in the preceding paragraph.

Another problem is evident from the data in Table 3 wherein the strain control test data with mean strain are listed. If the Langer assumptions were true for Alloy 718, then the mean stress at half cycle life should reach an upper saturation value; however, actual observation shows the mean stress to be related to the mean strain. Figure 7 illustrates some of the hysteresis loops from two actual tests. The loops show that a considerable mean stress persists even though some degree of inelastic behavior is present. The amount of mean stress retained appears to be related to the prior deformation in that the higher the mean strain, the longer the mean stress persists. More relaxation was noted with tests with lower mean strains (see Figure 7b). Data comparing strain control tests at 427°C both with and

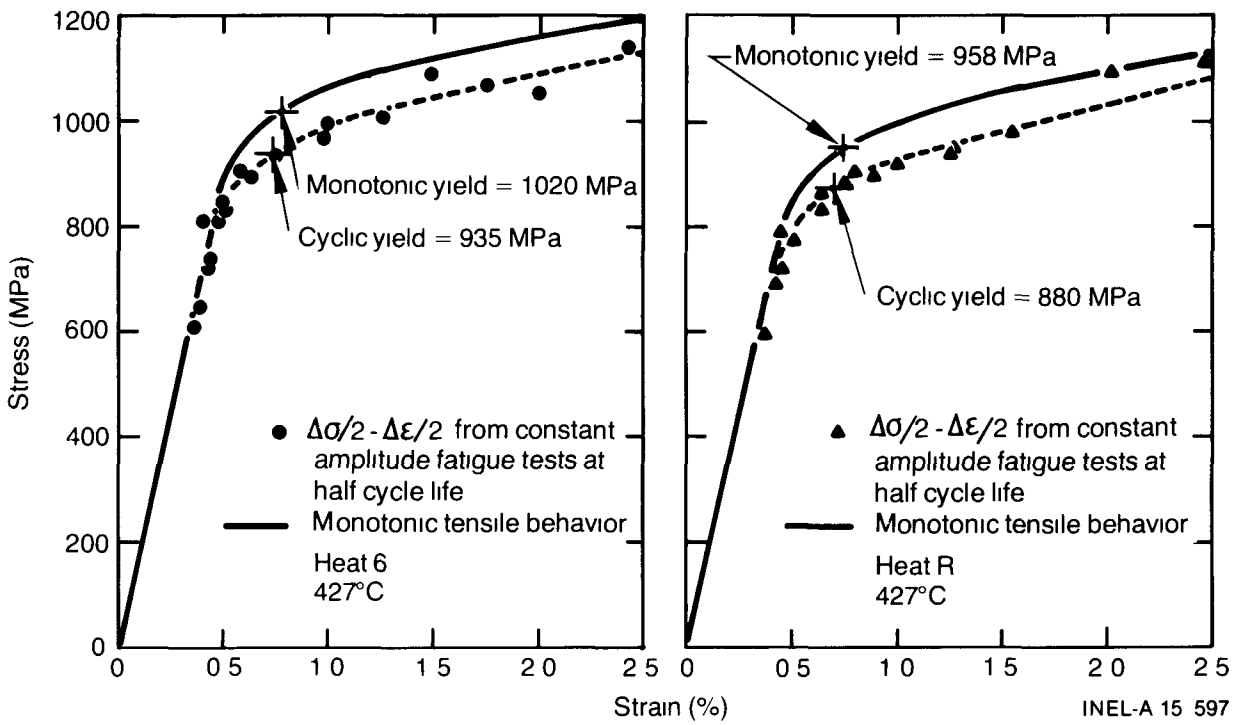

Figure 6. Stress-strain curves for heats 6 and R at 427°C comparing cyclic and monotonic behavior.

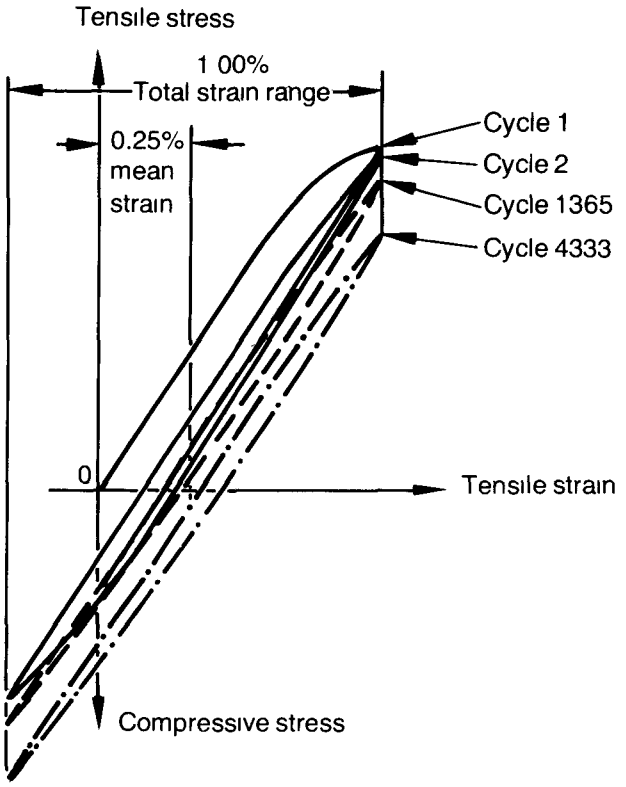

(a) Specimen 614-11, 1 00% total strain range with 0 25% mean strain

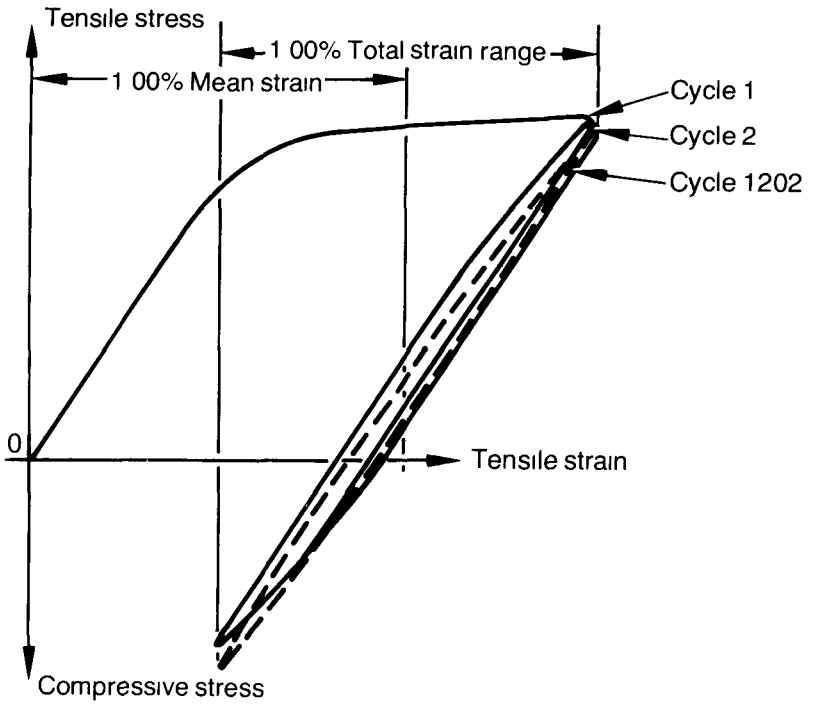

(b) Specimen 625-46, 1 00% total strain range with 1 00% mean strain

INEL A-15 592

Figure 7. Hysteresis loops of Alloy 718 strain-controlled fatigue tests with mean strain. Test temperature: 427°C.

without mean strains are shown in Figure 8. Except for the tests with 1.00% mean strain, the cycle lives did not appear to have been greatly affected by the mean strain. The results therefore support the Langer assumptions even though a mean strain persisted when inelastic behavior was present.

A third difficulty with the Modified-Goodman approach is properly accounting for mean stresses in load (or stress) control situations. It is possible to cycle Alloy 718 in load control at temperatures below the creep range with a large mean stress such that the peak tensile stress approaches the ultimate tensile strength and yet the cyclic stresses can be totally elastic after the first quarter cycle. This type of mean stress loading is not included in the Langer assumptions. Specimen R11-7 (Table 2) is an example of a test where the peak stress was very near the ultimate tensile strength. In fact, another specimen run at the same loads failed in the first cycle.

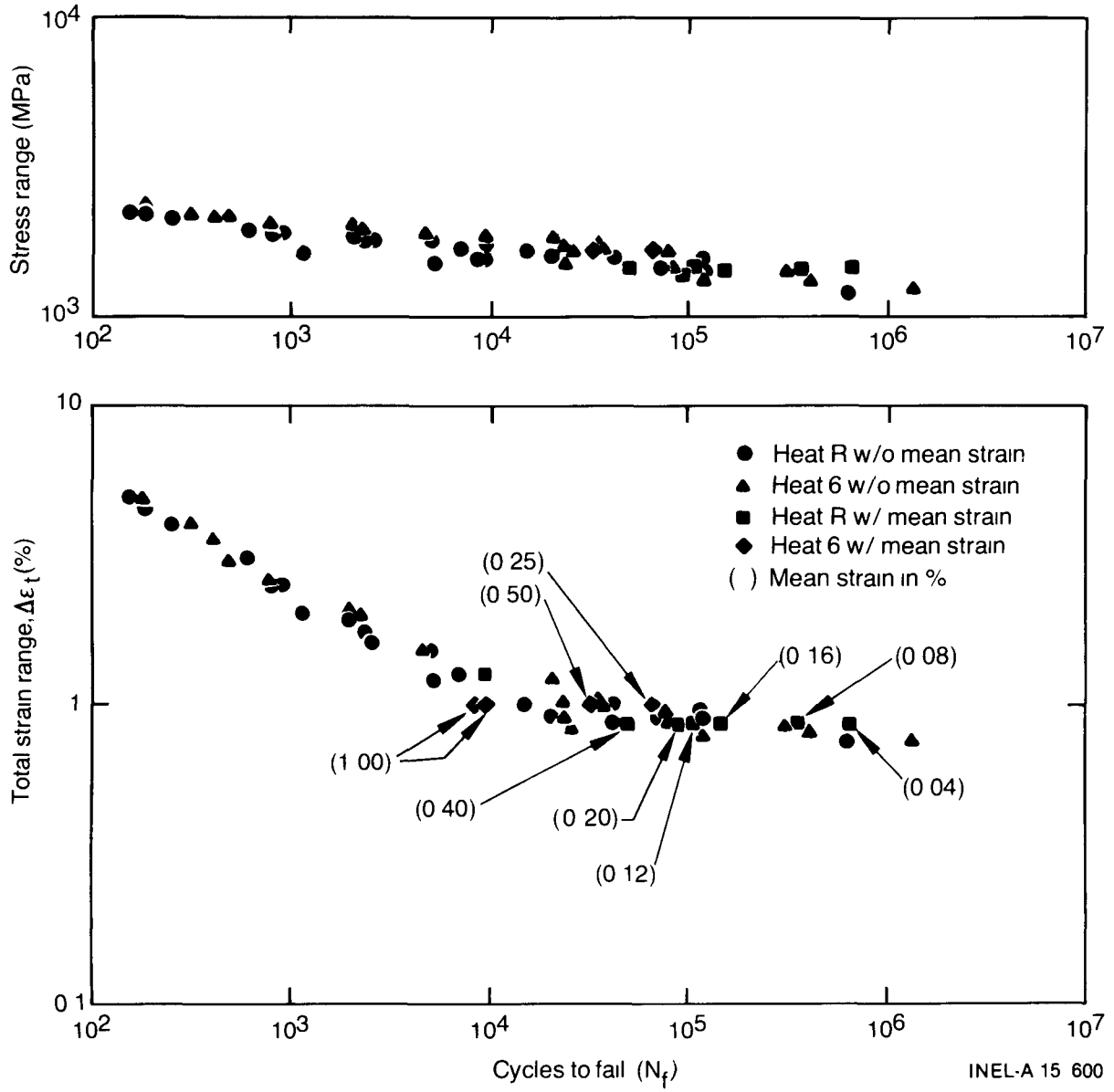

Figure 8. Strain-controlled fatigue of Alloy 718 at 427°C showing effects of mean strain on stress range and cycle life.

Another model that has been proposed to correct for mean stresses is the Peterson cubic equation[10] and is described as:

$$S_{eq} = \frac{7\,S_a}{8 - \left[1 + \frac{S_m}{S_u}\right]^3} \qquad (3)$$

where the symbols are the same as identified previously. To put it in the same format as the Modified-Goodman correction equation [Eq. 2], it should be written as:

$$S_a = \frac{S_{eq}\left(8 - \left[1 + \frac{S_m}{S_u}\right]^3\right)}{7} \qquad (4)$$

The cubic model is similar to the linear Modified-Goodman model and can be drawn on the same type of diagram. The cubic model is a third-order curve that lies above the linear model and predicts a less severe effect of mean stress.

Another model that has been proposed to correct for mean stresses is the equivalent strain parameter model proposed by Smith et al.[11] and is described as:

$$\varepsilon_{eq} = (\varepsilon_a)^m\,(S_{max}/E)^{1-m} \qquad (5)$$

where

ε_{eq} = equivalent strain parameter

ε_a = strain amplitude

S_{max} = maximum stress

E = the elastic modulus

m = a constant between 0 and 1.

When ε_a is nominally elastic, as it is in the case of Alloy 718 in high-cycle fatigue, then Equation (5) can be written as:

$$S_{eq} = \varepsilon_{eq}E = (S_a)^m\,(S_{max})^{1-m} \qquad (6)$$

where S_{eq} is now the equivalent-stress parameter, or the cyclic stress amplitude equivalent in cycles-to-fail, N_f, to a zero mean stress test. S_a is the stress amplitude of the mean stress test. If $S_{max} = S_a + S_m$ and m = 0.5, then

$$S_{eq} = \sqrt{S_a\,(S_a + S_m)} \qquad (7)$$

When $S_m = 0$, then $S_{eq} = S_a$. Letting m = 0.5 gives a good correlation in some aluminum alloys, AISI 1015, 1045, and 4340 steels,[11] and cast bronze alloys.[12] Equation (7) has become known as the stress-strain parameter.

To compare these models with actual Alloy 718 test data it is necessary to normalize the data and models so all heats, test temperatures, and cycle lives can be plotted together. As the models are now described, a separate diagram is needed for each value of N_f. For the linear and cubic mean stress models, a normalized Modified-Goodman diagram (S_a/S_{eq} versus S_m/S_u)was used. For the stress-strain parameter, a plot of S_a/S_{eq} versus S_m/S_{eq} was used. The linear and cubic models are readily normalized by rearranging.

$$\text{Linear:}\quad \frac{S_a}{S_{eq}} = 1 - \frac{S_m}{S_u} \qquad (8)$$

$$\text{Cubic:}\quad \frac{S_a}{S_{eq}} = \frac{8 - \left[1 + \frac{S_m}{S_u}\right]^3}{7} \qquad (9)$$

The stress-strain parameter can be normalized by first squaring both sides and rearranging to give

$$\frac{S_a^2}{S_{eq}^2} + \frac{S_a\,S_m}{S_{eq}\,S_{eq}} - \frac{S_{eq}^2}{S_{eq}^2} = 0 \qquad (10)$$

and then solving the resulting quadratic equation to obtain

$$\frac{S_a}{S_{eq}} = \frac{-\frac{S_m}{S_{eq}} + \sqrt{\left(\frac{S_m}{S_{eq}}\right)^2 + 4}}{2} \qquad (11)$$

The S_a, S_m, and N_f values recorded during the mean stress experimental tests are listed in Table 2. For each mean stress (N_f), an equivalent S_{eq} value was obtained from a zero mean stress failure fatigue curve for the same heat of material at the same test temperature. These baseline data can be described by a three-parameter equation of the form:

$$S_{eq} = A\, N_f^{-c} + B \tag{12}$$

where A, B, and c are constants resulting from a cycle-decade-weighted,[a] nonlinear, maximum slope and pattern search regression analysis performed by Snow.[13] The resulting best-fit equations were normalized to room temperature and all strain control results were converted to stress amplitude using the relationship

$$S_{eq} = \Delta\varepsilon_t / 2E \tag{13}$$

where $\Delta\varepsilon_t$ is total strain range and E is the room temperature Young's modulus [199.95 GPa (29.0 x 10^6 psi)]. The resulting S_{eq} value is a fictitious value when inelastic behavior is present, but this is the common convention used by the ASME Boiler and Pressure Vessel Code and is easily converted back to strain values using just one multiplying factor. The constants used in determining the baseline equations are given in Table 4. A temperature correction factor, also listed in Table 4, was used to correct the calculated S_{eq} values to the appropriate test temperature.

Similarly, the S_u value, used to normalize the mean stress value for the Goodman diagrams, was obtained for the heat/test-temperature combination. Where such S_u data were not available, a representative value was chosen. Table 4 lists the values used.

In general, mean stress fatigue data were used only if the number of cycles to failure was greater than 50,000. Tests with lower cyclic lives often involved some degree of plastic flow on each cycle. Under these circumstances, the assumed linear relationship between stress and strain is incorrect. A total of 76 valid mean stress data points were used in the analysis.

Mean stress tests which did not result in failure are included in the data base. In general, the actual failure points would lie farther out (from the origin) than the point that was plotted. Thus, the use of nonfailure points is clearly conservative.

Figure 9 contains a Modified-Goodman plot of all of the mean stress data. The linear and cubic model prediction lines are also shown. The trend of the data fits the linear representation fairly well between S_m/S_u values of 0.1 and 0.4, but above this range the linear model is clearly conservative. The cubic model passes through some of the data but really does not fit the trend. At S_m/S_u values between 0.1 and 0.5, a number of data points fall significantly below the cubic prediction. At higher S_m/S_u values (> 0.6) both the linear and cubic models appear to be conservative. In Figure 10, the stress-strain parameter predictions are compared to the data. The stress-strain parameter appears to match the trend of the data very well over an extremely wide range of S_m/S_{eq} values. In Figure 11, actual data for one temperature and one heat are compared with the best-fit curve for no mean stress and the stress-strain parameter correction for a S_{max} of 758 MPa (proportional limit for the reference heat at 427°C). Stress values were converted to strain in Figure 11 using an elastic modulus of 173.5 GPa.

The stress-strain parameter also indicates a stress amplitude threshold below which no failure will occur regardless of the mean stress value. A limiting value of mean stress will be reached, of course, when the sum of the stress amplitude and mean stress is equal to the ultimate tensile strength. This threshold phenomenon also appears to be confirmed by the experimental data. No failures were experienced at the 427°C test temperature when the stress amplitude was below approximately 260 MPa, even though some peak stresses were near or just below the ultimate tensile strength. Figure 12 gives evidence of the stress amplitude threshold effect where the stress amplitude reduction factor due to mean stress, S_a/S_{eq}, is plotted against S_{max}. A lower-bound envelope drawn through the data shows that the reduction factor decreases in an essentially linear fashion until a value of approximately 0.5 is

a The cycle-decade-weighted technique gives equal weight to each life decade (10^1—10^2, 10^2—10^3, 10^3—10^4, etc.) regardless of the number of data points in each decade. This method inhibits the tendency of the greater volume low-to-intermediate life data to unduly bias the curve in the high-cycle regime where data are more sparse

TABLE 4. MATERIAL PROPERTIES USED IN MEAN STRESS EVALUATIONS

Heat Number[a] (Index)	Temperature (°C)	Ultimate Tensile Strength (S_u) (MPa)	Fatigue Equation Parameters[b] A (psi)	B (psi)	C	Temperature Correction Multiplication Factor
Heat R (1.3)	24	1364	15.074×10^6	70,794	0.555	1.000
	427	1215	3.894×10^6	68,490	0.382	0.890
	649	1106	1.221×10^6	66,955	0.300	0.815
Heat 6 (1.4)	427	1213	4.869×10^6	71,347	0.410	0.890
Heat 2 (1.13)	24	1382	2.376×10^6	52,338	0.326	1.000
	649	1147	1.366×10^6	107,088	0.370	0.815

a. Heat Index is identification as used by Snow in Reference 13.
b. These fatigue equation parameters (from Reference 13) are from tests only for this heat/test temperature combination. After calculating S_{eq} and correcting for temperature it was converted to MPa by multiplying by 6.8948×10^{-3}.

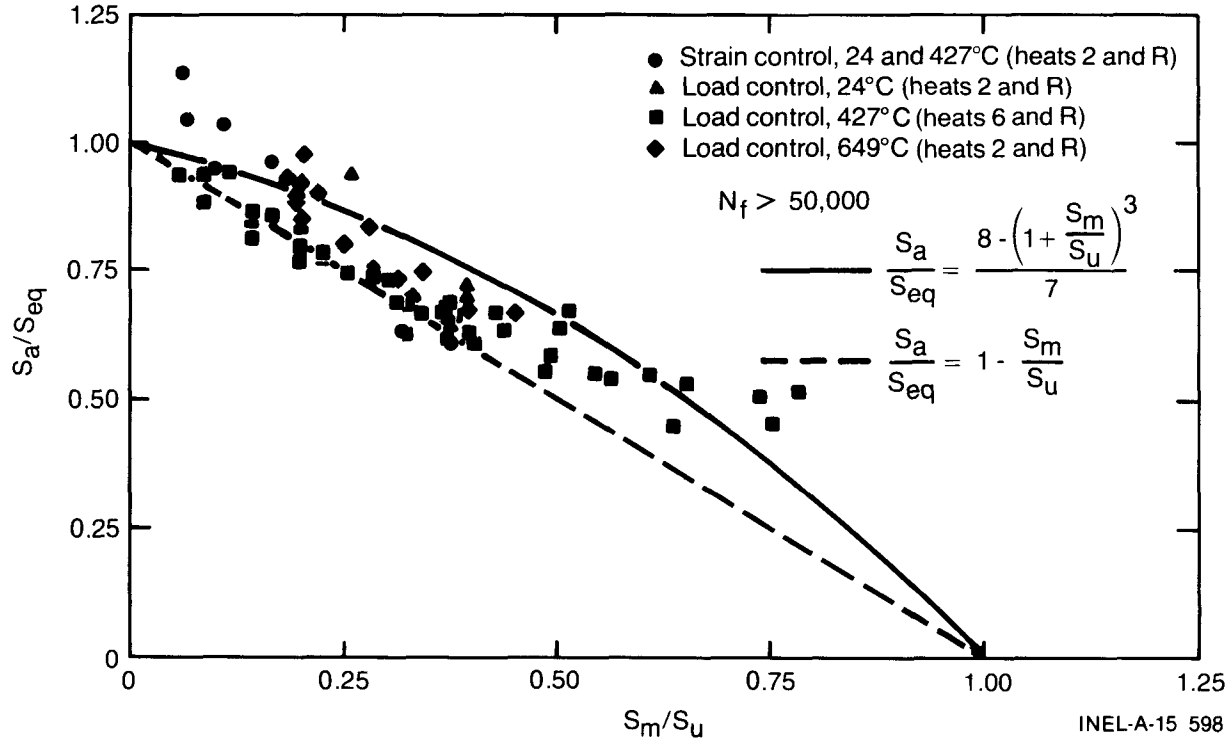

Figure 9. Mean stress fatigue data of Alloy 718 compared to the Peterson cubic and the Modified-Goodman linear models.

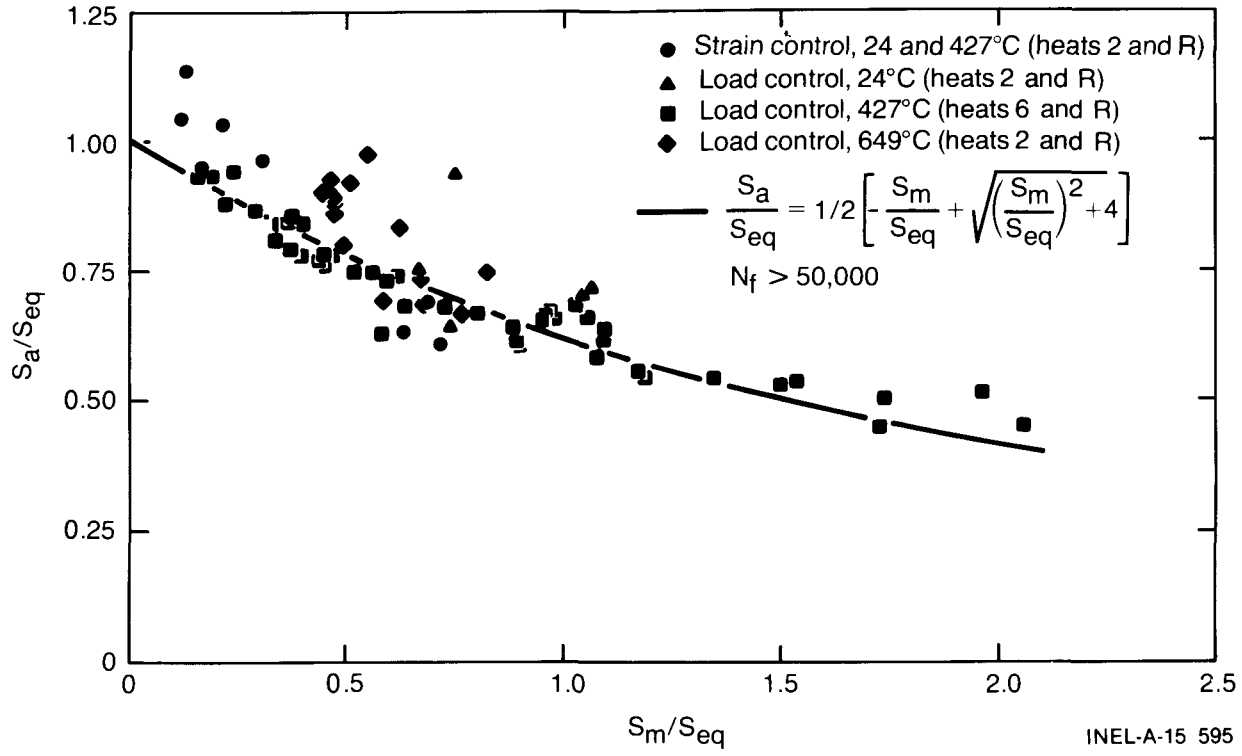

Figure 10. Mean stress fatigue data of Alloy 718 compared to the stress-strain model.

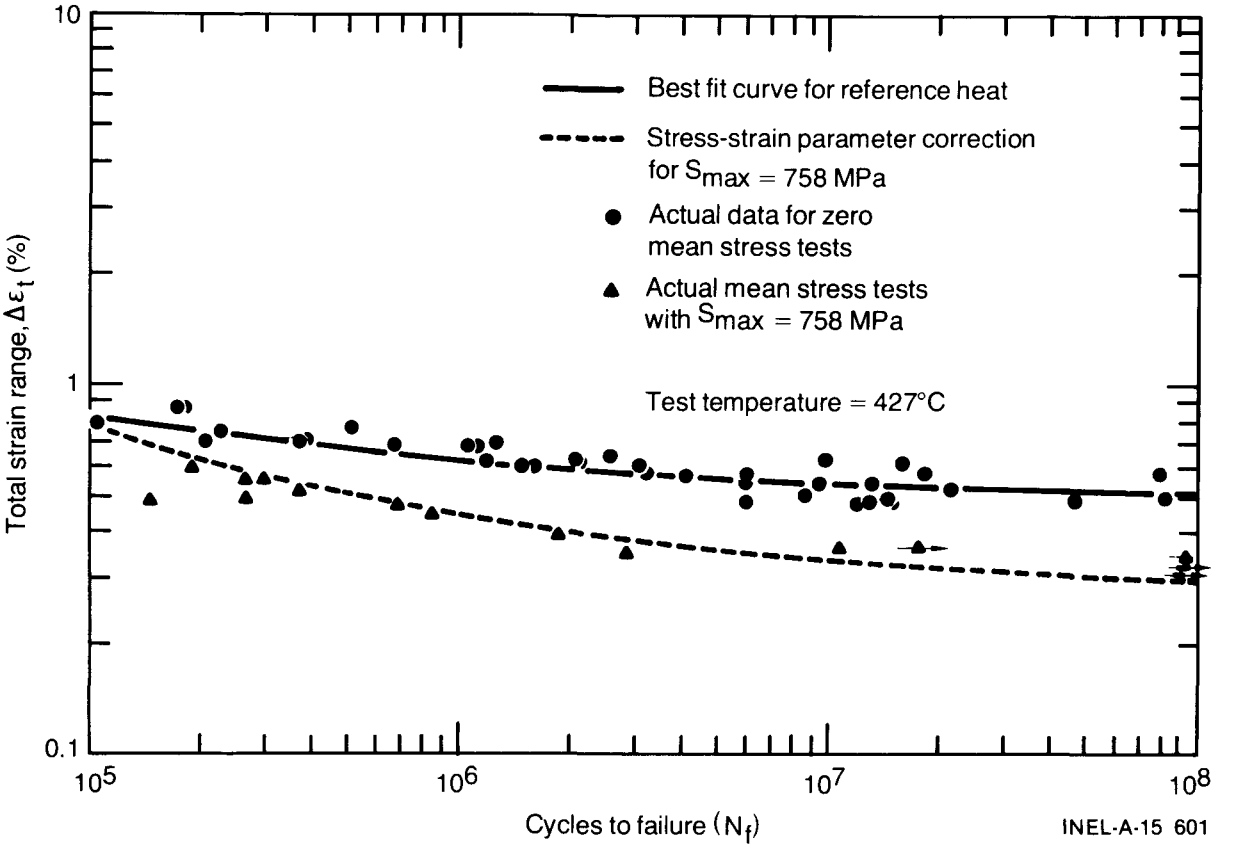

Figure 11. Comparison of actual fatigue test data of Alloy 718 at 427°C with stress-strain parameter predictions.

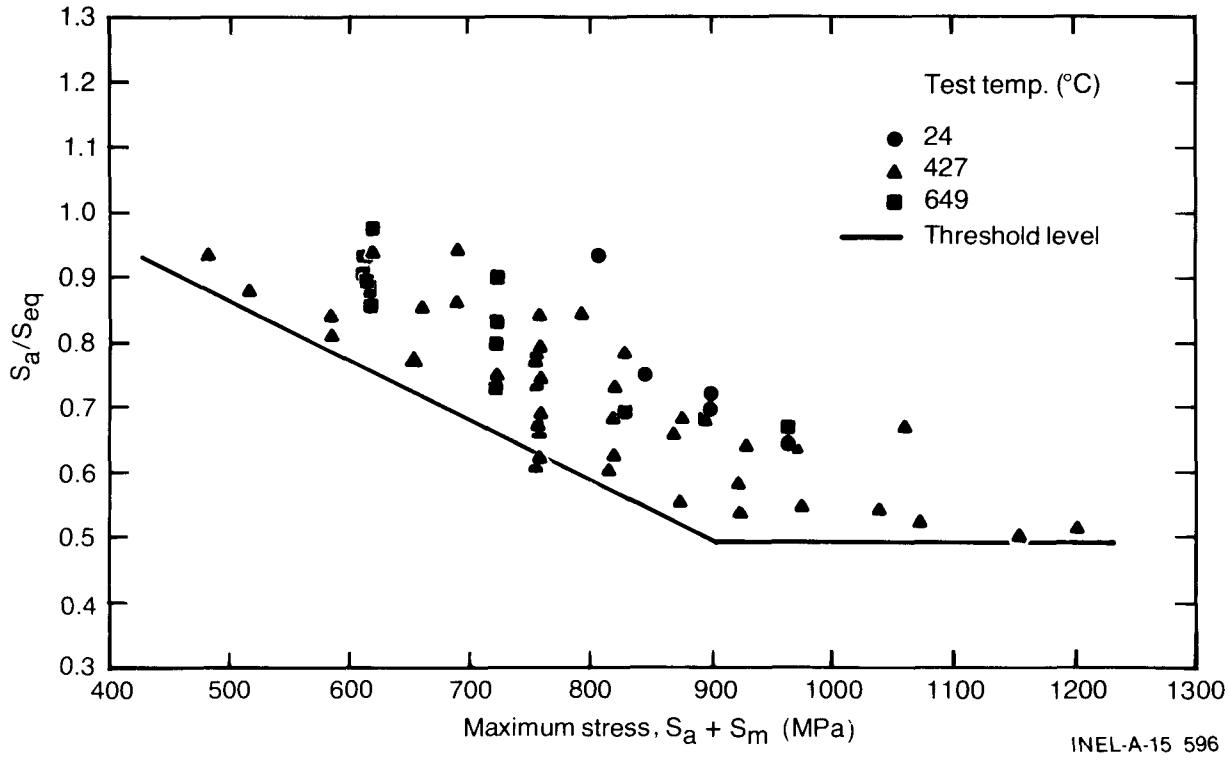

Figure 12. Stress amplitude reduction versus maximum stress for Alloy 718 mean stress tests.

reached and then levels off, showing no further decrease even though the maximum stress continues to increase right up to the ultimate tensile strength. This lower-bound line is really a bilinear approximation of a minimum stress-strain parameter curve. Although data substantiating the stress amplitude threshold phenomenon are not plentiful, all available data support the observation. At higher temperatures, in the creep regime, the stress amplitude threshold may very well be dominated by cyclic creep effects (ratcheting) when peak stresses are above the proportional limit.

CONCLUSIONS

From the mean stress tests conducted and the subsequent analysis the following conclusions concerning the effects on high-cycle fatigue of Alloy 718 are made:

1. Tensile mean stress does result in a significant decrease in the cyclic stress amplitude that can be sustained by this material.
2. When testing at temperatures in the creep regime and at peak stresses above the proportional limit, stress relaxation is observed in strain control tests and ratcheting is observed in load control tests.
3. The linear Modified-Goodman model predicts mean stress effects fairly well at low-to-moderate mean stresses, but the stress-strain parameter best fits the data trend over the entire range of possible mean stresses. The Peterson cubic model does not fit the test data at all. It is recommended that the stress-strain parameter be used to predict mean stress effects of Alloy 718.
4. There appears to be a stress amplitude threshold, at least at temperatures up to 427°C, below which no failures will occur regardless of the maximum stress right up to the ultimate tensile strength.

REFERENCES

1. C. R. Brinkman and G. E. Korth, "Strain Fatigue and Tensile Behavior of Inconel 718 from Room Temperature to 650°C," *Journal of Testing and Evaluation 2*, 4, July 1974, pp. 249-259.

2. G. E. Korth and G. R. Smolik, *Status Report of Physical and Mechanical Test Data of Alloy 718*, TREE-1254, March 1978.

3. G. E. Korth and G. R. Smolik, *Mechanical Property Program of Alloy 718, "Mechanical Properties Test Data for Structural Materials Quarterly Progress Report for Period Ending April 30, 1978,"* ORNL-5416, pp. 2-21.

4. G. E. Korth and G. R. Smolik, *Mechanical Property Program of Alloy 718, "Mechanical Properties Test Data for Structural Materials Quarterly Progress Report for Period Ending July 31, 1978,"* ORNL/BRP-78/2, pp. 1.1-1.10.

5. G. E. Korth, J. E. Flinn, G. R. Smolik, *Mechanical Property Program of Alloy 718, "Mechanical Properties Test Data for Structural Materials Semiannual Progress Report for Period Ending January 31, 1979,"* ORNL/BRP-79/1, pp. 1.1-1.51.

6. G. R. Smolik and G. E. Korth, *Evaluation of Roll-Extruded Alloy 718 Tubing*, TREE-1255, May 1978.

7. G. E. Korth, J. E. Flinn, G. R. Smolik, *Mechanical Property Program of Alloy 718, "Mechanical Properties Test Data for Structural Materials Semiannual Progress Report for Period Ending July 31, 1979,"* ORNL/BRP-79/5, pp. 1.1-1.26.

8. B. F. Langer, "Design of Pressure Vessels for Low-Cycle Fatigue," *Journal of Basic Engineering*, Transactions of ASME, Series B,*84*,3, September 1962, pp. 389-402.

9. C. E. Jaske and W. J. O'Donnell, "Fatigue Design Criteria for Pressure Vessel Alloys," *ASME Paper No. 77-PVP-12.*

10. R. E. Peterson, "Brittle Fracture and Fatigue in Machinery," *Fatigue and Fracture of Metals*, New York: John Wiley & Sons, 1952.

11. K. N. Smith, P. Watson, T. H. Topper, "A Stress-Strain Function for Fatigue of Metals," *Journal of Materials, 5*, 4, December 1970, pp. 767-778.

12. C. E. Jaske, D. A. Utah, W. K. Boyd, "Corrosion Fatigue of Cast Propeller Alloys," Propellers '78, S-6, Published by the Society of Naval Architects and Marine Engineers, New York, New York, 1979, pp. 4-1 to 4-28.

13. A. L. Snow, Westinghouse Electric Co., Advanced Reactors Division, Madison, PA, Unpublished report, February 1980.